Top Catal (2017) 60:997–1008
DOI 10.1007/s11244-017-0765-5

ORIGINAL PAPER

Selective Hydrogenation of Acetylene Over Pd/Al_2O_3 Catalysts: Effect of Non-thermal RF Plasma Preparation Methodologies

Yanan Li[1,2] · Ben W.-L. Jang[1]

Published online: 6 April 2017

Abstract Supported palladium nanocatalysts have been reported to be active in selective hydrogenation of acetylene. In this work, non-thermal radio frequency plasma modification has been applied to Pd/Al_2O_3 catalysts for selective hydrogenation of acetylene in the presence of excess ethylene. High ethylene selectivity, good acetylene conversion activity and high *TOF* were obtained on the plasma-treated catalysts. To understand the plasma effect, the catalysts were characterized by differential scanning calorimetry in hydrogen (H_2-DSC), pulse H_2 chemisorption, X-ray photoelectron spectroscopy (XPS) and temperature-programmed desorption with ethylene (C_2H_4-TPD) experiments. XPS and H_2-DSC results confirmed that the Pd precursor could be effectively reduced to the metallic state during the room temperature plasma treatment. Plasma treatment also improved the dispersion of Pd particles with strong interaction between Al_2O_3 support and PdO and Pd nitrate precursors. In addition, C_2H_4-TPD indicated that plasma treatment could lead to an enhanced catalytic performance on selective hydrogenation of acetylene. It demonstrates that the non-thermal RF plasma treatment is an effective way to manipulate surface properties and the interaction between metals and supports of supported Pd catalysts for selective hydrogenation.

✉ Yanan Li
liyan.sshy@sinopec.com

✉ Ben W.-L. Jang
Ben.Jang@tamuc.edu

[1] Department of Chemistry, Texas A&M University-Commerce, Commerce, TX 75429-3011, USA

[2] SINOPEC Shanghai Research Institute of Petrochemical Technology, Shanghai 201208, People's Republic of China

Keywords Palladium catalyst · Aluminum oxide · Plasma · Strong metal-support interaction (SMSI) · Acetylene hydrogenation

1 Introduction

During the production of ethylene by naphtha cracking, it is accompanied by impurity of acetylene which is detrimental to the catalytic ethylene polymerization processes. Selective hydrogenation of acetylene to reduce acetylene to 5–10 ppm range in an excess of ethylene stream is highly desirable for the industrial process to purify the alkene streams [1–4]. Apparently, the critical requirements in this process are (i) to achieve high selectivity to ethylene at high conversions; (ii) to minimize hydrogenation of the alkene streams at high conversions; and (iii) to achieve long durability against deactivation via carbonaceous deposits formation [5]. It is well known that palladium (Pd) catalysts are effective to selectively hydrogenate acetylene to ethylene [6, 7]. However, Pd catalysts suffer from poor selectivity when ethylene is hydrogenated to ethane which simultaneously leads to an unwanted decline of the ethylene selectivity producing a large amount of undesirable ethane [8]. A number of studies have reported the factors that influence the selectivity, which include Pd particle size and dispersion [4, 9, 10], choice of catalyst precursor and support [3, 11], addition of various promoters [12–14], kinetic effects [15–17] or polymeric species on the catalyst surface [18, 19]. The surface structure of Pd catalysts, such as particle size, plays a considerable role on the selective hydrogenation of acetylene in the presence of ethylene. In order to maintain the well dispersed metal particle in the catalyst structure, a variety of efficient methods have been developed [20, 21]. Savithra et al. [22] reported the

encapsulation-reduction method in colloidal state to fabricate the Pd-P nanoparticles with precisely controlled particle size of 5–10 nm. Tsung et al. [23] combined the acetic acid mediated sol–gel chemistry with the aerosol-assisted evaporation-induced self-assembly approach to fabricate mesoporous ZrO_2, Al_2O_3 and TiO_2 submicrospheres with highly crystallized framework.

Non-thermal plasma-based techniques for catalyst preparation have recently attracted significant attention for catalyst design and development [24–30]. It has been observed in our laboratory that, with the non-thermal radio frequency (RF) plasma treatment, the supported Pd, Ag, Au, Ni catalysts exhibited an enhanced reaction activity and stability compared to the untreated counterpart [29–34]. RF plasma, known as conventional non-thermal plasma process at room temperature, is consist of ionized gaseous substance, including electrons, ions, and neutral particles which possess the ability to distribute energy. It has been reported RF plasma is an effective way to gain high supported metal dispersion, strong metal–support interfaces and manipulate the surface properties of catalysts. Therefore, it is widely applied in the preparation of heterogeneous catalysts and synthesis of nanostructure materials [35–38].

In this work, we focus on the investigation of Pd/Al_2O_3 catalysts with non-thermal RF plasma treatment preparation method and compare the activity of selective hydrogenation of acetylene over the H_2, Ar and O_2 plasma treated Pd/Al_2O_3 catalysts. In previous work [31, 39], we had already confirmed that the Pd catalysts supported on the reducible TiO_2 showed higher metal dispersion, enhanced metal–support interaction and better catalytic performance for acetylene hydrogenation. Since Pd/Al_2O_3 catalysts have been used worldwide for acetylene selective hydrogenation industrial processes, it is more practical to explore the industrial Pd/Al_2O_3 catalysts' performance employed plasma treatment. In order to bring more insight into the beneficial effect on industrial Pd/Al_2O_3 catalysts induced by plasma treatment, various characterizations including H_2-DSC, H_2-chemisorption, XPS and C_2H_4-TPD were applied to examine the prepared catalysts. Based on the experimental results, the catalyst improvements are discussed for the selective hydrogenation of acetylene, and to evaluate the hydrogenation performance of plasma treated Pd/Al_2O_3 catalysts.

2 Experiment

2.1 Catalyst Preparation

1/8 inch aluminum oxide pellets (γ-Al_2O_3, Alfa Aesar) were crushed and sieved through 20–40 mesh sieves. The screened support particles were then dried at 200 °C for 10 h followed by cooling down to room temperature. The 0.05 wt% (500 ppm), 0.2 and 1 wt% supported Pd catalysts were impregnated for 12 h by incipient wetness impregnation methods with solution of palladium nitrate (Alfa Aesar) then dried at 120 °C in air for 12 h. The obtained conventional samples are denoted as Pd/Al_2O_3-C and used as prepared. Some Pd/Al_2O_3-C samples were treated by non-thermal RF plasma as discussed below, and some Pd/Al_2O_3-C samples were calcined in the air at 500 °C for 2 h.

2.2 Plasma Treatment

Plasma treatments for the fresh Pd/Al_2O_3-C catalysts were carried out in the custom-designed 360° rotating RF plasma system. The details of the system and the apparatus schematic are described in a previous publication [32]. A system pressure of 400 mTorr was used for plasma treatments in this study. Typically, 0.5 g of catalysts was loaded into the plasma chamber for hydrogen, oxygen and argon plasma treatments. The duration of plasma treatment was set at 30 min with a continuous waveform of 130 W power. The samples with additional hydrogen, oxygen and argon continuous RF plasma treatment are designated as Pd/Al_2O_3-HP, Pd/Al_2O_3-OP and Pd/Al_2O_3-AP.

2.3 Catalysts Characterization

The thermal analysis of Pd/Al_2O_3 samples was carried out using a DSC apparatus: Q10 model TA instruments. The temperature was calibrated with a high-purity indium standard. Samples of approximately 5–8 mg were weighed with precision of 0.1 mg aluminum pans prior to analysis. An empty aluminum pan was used as the reference and the chamber was purged with UHP nitrogen (Matheson Tri-gas Industrial Gases) during analysis. Each sample underwent the procedure as: heating from room temperature to 120 °C then holding isothermal at 120 °C for 30 min, cooling equilibrated from 120 to −50 °C, and heating from −50 °C to the maximum temperature of 300 °C in 5 vol% H_2/N_2. The temperature scanning rate for all cycles was 15 °C/min. All the measurements were repeated at least three times.

Pulse H_2 chemisorption on the Pd/Al_2O_3 catalysts at 25 °C was performed with the AMI-200 automated system. Prior to the pulse H_2 chemisorption measurement, each sample was reduced in a 30 vol% H_2/Ar flow (30 mL/min) at 200 °C for 3 h with a ramping rate of 10 °C/min. The reduced sample was purged in UHP argon (Matheson Tri-gas Industrial Gases) at 200 °C for 1 h and then cooled down in argon atmosphere to desorb any hydrogen. The number of exposed palladium atoms on the surface was calculated by the total amount of hydrogen adsorption. The average dispersion of palladium crystallites was determined with 0.01% error limits for measurement accuracy

by the stoichiometric factor $H_2/Pd = 0.5$ [40], according to the total amount of H_2 chemisorbed on the Pd samples. The average Pd particle size (*d*) was estimated assuming as spherical crystallite. All the measurements were repeated at least three times.

XPS analysis of Pd/Al_2O_3 was performed using a Thermo Scientific K-Alpha XPS instrument operated with monochromatic Al Kα X-ray source (1486.7 eV) and a combined low energy Ar-ion/electron source for charge compensation. The conventional sample and the ones with additional hydrogen, oxygen and argon continuous RF plasma treatment were directly introduced into the analysis chamber through a turbo-pumped load-lock chamber without any thermal reduction treatment. The samples were directly pressed to a self-supported disk (10×10 mm^2), mounted onto a sample holder, and then degassed overnight in the vacuum chamber. Base pressure in the analysis chamber was 8×10^{-10} mbar. The contaminative C 1s peak at 284.6 eV was used for calibration.

A temperature-programmed desorption (TPD) study of Pd/Al_2O_3 was performed in the AMI-200 automated system using a downstream gas sampling quadrupole mass spectrometer (QMS, Pfeiffer-Balzers Omnistar™) equipped with gas sampling capillary followed by an apertured entrance into the turbo-pumped QMS chamber. Approximately 0.030 g of catalysts were placed in a quartz tube and first reduced in 4 vol% H_2/He (mixture of UHP hydrogen and UHP helium from Matheson Tri-gas Industrial Gases) flow at 30 mL/min for 1.5 h at 200 °C (using a ramp rate of 30 °C/min) followed by flushing in UHP helium (Matheson Tri-gas Industrial Gases) for 30 min. Then the catalysts were cooled down to −50 °C under helium flow. The catalyst surface was saturated with ethylene by applying a high purity grade ethylene at 10 mL/min for 30 min followed by helium flushing. The temperature-programmed desorption was performed in helium with a constant heating rate of 20 °C/min from −50 to 200 °C. The amount of desorbed ethylene was measured by the on-line mass spectrometer. The signal of C_2H_4 ($m/z = 27, 28$) were continuously monitored and used for the TPD analysis.

2.4 Reaction Tests

All catalysts were tested for the selective hydrogenation of acetylene. A 1/4 inch quartz reactor (i.d., 4 mm) housed in a GC oven with temperature-programmed heating and cooling capabilities at low-temperature ranges was used. Normally, the conventional catalysts were reduced in UHP hydrogen (Matheson Tri-gas Industrial Gases) at 200 °C for 30 min and then underwent purging with UHP nitrogen (Matheson Tri-gas Industrial Gases) at room temperature before the reaction testing was done. A temperature-programmed procedure with a 0.2 °C/min ramping rate was used to test the catalytic performance of Pd/Al_2O_3. A gaseous mixture containing 5/1, 3/1 and 2/1 H_2/C_2H_2 molar ratios (mixture of 1.14 vol% C_2H_2 in C_2H_4 from Scott Specialty Gases and UHP H_2 from Matheson) was fed into the reactor at a space velocity of 90,000 mL/h/g. All flows were delivered by mass flow controllers. The analysis of the gas components from the microreactor was performed by an on-line Shimadzu GC 17 A equipped with a 30 m × 0.32 mm (i.d.) × 1.50 µm GS-CARBONPLOT capillary column operating at 80 °C and a FID detector.

Possible products for acetylene hydrogenation are ethylene and ethane. Due to the extreme high concentration of ethylene and small concentration of acetylene in the feed gas, if the calculation of ethylene selectivity is based on the difference of ethylene concentrations before and after the reaction, the error will be undoubtedly high. Therefore, in this study, the calculation of ethylene selectivity is based on the production of ethane. The acetylene conversion, the acetylene selectivity to ethylene, the ethylene yield and the turnover frequency (*TOF*) for acetylene hydrogenation are defined as follows. Selected reaction conditions were used for stability tests [41].

$$Conversion\ (\%) = \frac{C_2H_2(\text{feed}) - C_2H_2}{C_2H_2(\text{feed})} \times 100\% \quad (1)$$

$$Selectivity\ (\%) = 1 - \frac{C_2H_6 - C_2H_6(\text{feed})}{C_2H_2(\text{feed}) - C_2H_2} \times 100\% \quad (2)$$

$$\text{Yield}\ (\%) = \text{Conversion}\ (\%) \times \text{Selectivity}\ (\%) \quad (3)$$

$$TOF = \frac{\text{Rate of } C_2H_2 \text{ consumption } (s^{-1})}{\text{No. of exposed Pd sites on the catalyst}} \quad (4)$$

3 Results and Discussion

3.1 Reaction Performance of Conventional Pd/Al_2O_3-C Catalysts

3.1.1 Comparison of Different H_2/C_2H_2 Ratios Over 1 wt% Pd/Al_2O_3-C

The acetylene conversion, selectivity of ethylene and ethylene yield of 1 wt% Pd/Al_2O_3-C catalyst at different H_2/C_2H_2 ratios are summarized in Fig. 1. In these cases, gaseous mixtures with a total flow rate of 90,000 mL/h/g at H_2/C_2H_2 ratios of 5/1, 3/1 and 2/1 were passed over the catalyst bed and the temperature was varied in the range of 25–75 °C. The initial conversion of 1 wt% Pd/Al_2O_3-C sample with H_2/C_2H_2 ratio of 5/1 and 3/1 were 16.5 and 16.4% at 25 °C and increased faster with elevated temperature than that with the H_2/C_2H_2 ratio of 2/1. The corresponding T_{50} values for the hydrogenation reaction on the

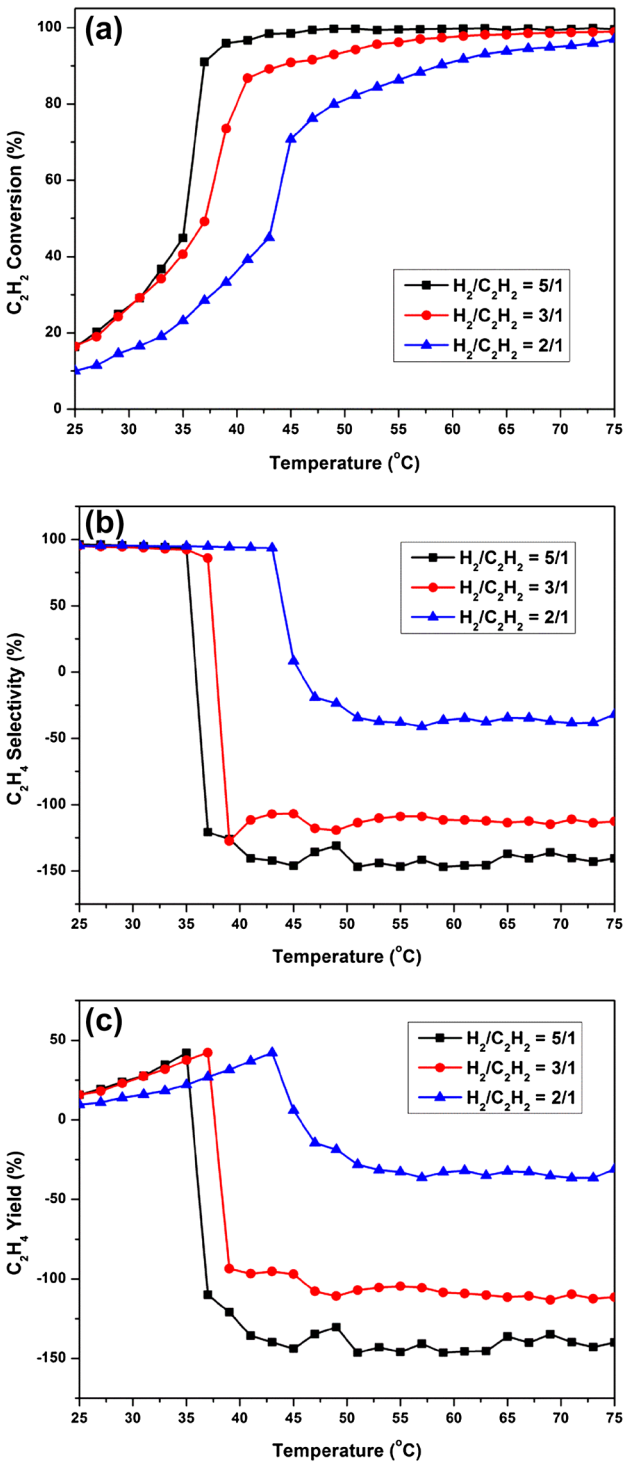

Fig. 1 Catalytic performance including **a** conversion, **b** selectivity and **c** yield of 1 wt% Pd/Al_2O_3-C catalyst with 5/1, 3/1 and 2/1 H_2/C_2H_2 ratios. GHSV = 90,000 mL/h/g

catalysts at H_2/C_2H_2 ratio of 5/1, 3/1 and 2/1 were 35.2, 37.1 and 43.4 °C, respectively. It could be found that the conversion at different H_2/C_2H_2 ratios followed the order of 5/1 > 3/1 > 2/1. These results demonstrated that increasing the H_2 partial pressure in the feed could promote the reaction process, and eventually lower the reaction temperature required to reach the same conversion [30, 42]. Sheth et al. [43] showed, by computation, that the acetylene reacts with the surface-bound atomic hydrogen on Pd(111) surface, which are formed favorably with high partial pressure of hydrogen. Therefore, higher partial pressure of hydrogen during the reaction with H_2/C_2H_2 ratio of 5/1 accelerated the acetylene hydrogenation on the Pd particles with higher conversion.

In the case of 5/1 and 3/1, the conversion reached 90.0% at the temperature below 45 °C. However, the ethylene selectivity shown in Fig. 1b cross over from positive to negative at lower temperature around 37 °C. Since the selective hydrogenation of acetylene is a typical consecutive reaction with over-hydrogenation forming ethane, the sharp selectivity drop was due to the fact that hydrogenation of ethylene formed and the existing ethylene in the feed to ethane is faster than the hydrogenation of acetylene to ethylene. The reaction with 2/1 ratio showed relatively constant selectivity of 95.0% at lower temperature. With increasing reaction temperature, this undesired loss of ethylene took place at 45 °C. As reported in the literature [44], higher acetylene conversion is typically accompanied by lower selectivity during the acetylene hydrogenation. The main by-product ethane was formed from over-hydrogenation of ethylene produced or adsorbed from the feed stream. An increase in hydrogen partial pressure would enhance the over-hydrogenation that ethylene would hydrogenate to form ethyl and then desorbed as ethane [8]. Therefore, the reaction with the H_2/C_2H_2 ratio of 2/1 showed much better ethylene selectivity than the cases of H_2/C_2H_2 ratio of 5/1 and 3/1, as shown in Fig. 1b. In order to compare the overall effect of H_2/C_2H_2 ratio for the hydrogenation, the results of ethylene yield were shown in Fig. 1c. The reaction with H_2/C_2H_2 ratio of 2/1 achieved its maximum ethylene yield of 42.1% at 43 °C, whereas the similar yield of about 41.9 and 42.2% for 5/1 and 3/1 ratio, respectively. It can be assumed that high H_2/C_2H_2 ratio with large amount of H_2 molecules could cover the active adsorption sites on the Pd particles and simultaneously lead to over-hydrogenation of ethylene with hydrogen to an undesirable ethane. An optimal H_2/C_2H_2 ratio among these three ratios in the ethylene hydrogenation reaction should be 3/1 or 2/1 favored for the selectively hydrogenation reaction of acetylene.

3.1.2 Comparison of Different Pd Loadings

The catalytic performance of Pd/Al_2O_3-C catalysts with different Pd loadings at the H_2/C_2H_2 ratio of 2/1 is shown in Fig. 2. Pd/Al_2O_3-C catalysts showed increasing acetylene conversion with elevated temperature with the following activity order: 1 > 0.2 > 0.05 wt% (500 ppm) as shown

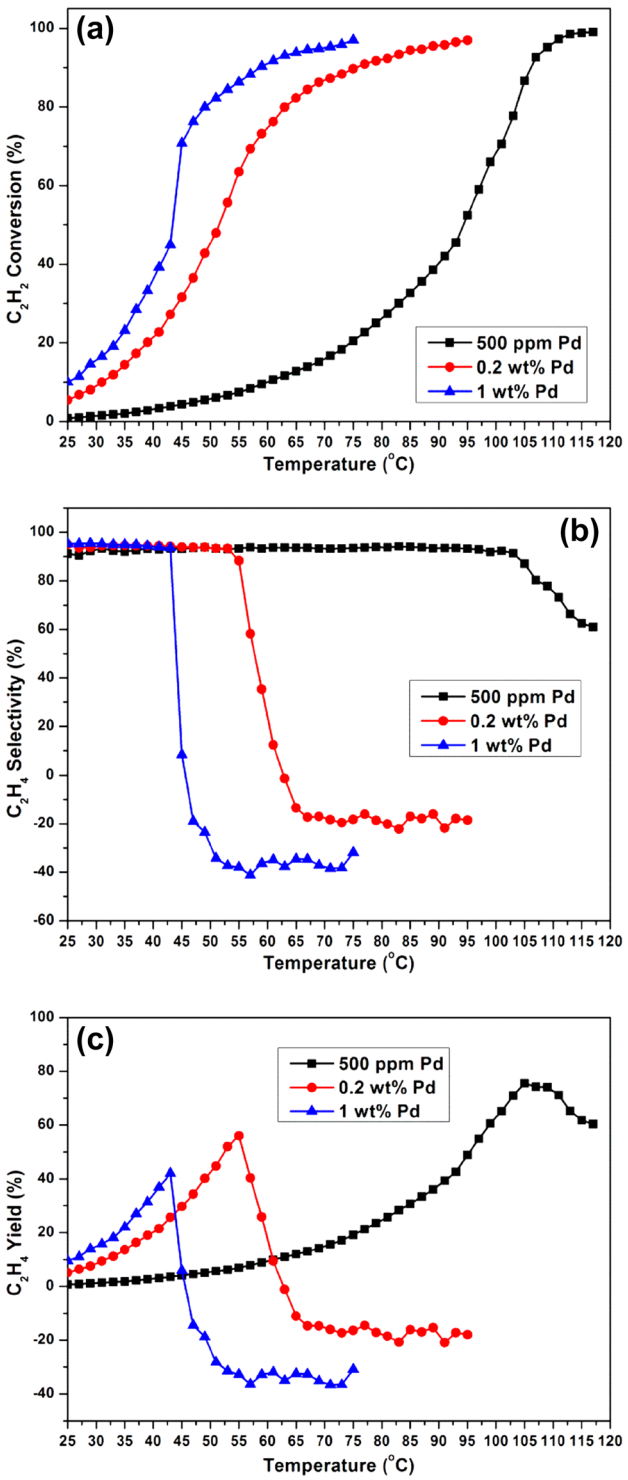

Fig. 2 Catalytic performance including **a** conversion, **b** selectivity and **c** yield of Pd/Al_2O_3-C catalyst with different Pd loadings. GHSV = 90,000 mL/h/g with the H_2/C_2H_2 ratio of 2/1

in Fig. 2a. With higher Pd loading of 0.2 and 1 wt%, the catalysts are much more active than the one with 0.05 wt% (500 ppm) Pd loading. The acetylene conversions at 45 °C were 4.4, 31.6 and 70.8% for the Pd/Al_2O_3-C catalysts with 0.05 wt% (500 ppm), 0.2 and 1 wt%, respectively.

Figure 2b shows the comparison of ethylene selectivity over three Pd/Al_2O_3-C catalysts. Both 1 wt% Pd/Al_2O_3-C and 0.2 wt% Pd/Al_2O_3-C catalysts presented relatively constant selectivity around 95.0 and 94.5%, respectively, at lower temperatures and then the ethylene selectivity decreased rapidly at higher temperatures. The reaction over 0.05 wt% (500 ppm) Pd/Al_2O_3-C catalysts showed the best selectivity behavior about 94.0% till 100 °C. The ethylene yield results are shown in Fig. 2c. The ethylene yield increased quickly at lower temperatures for 1 wt% Pd/Al_2O_3-C and 0.2 wt% Pd/Al_2O_3-C catalysts, reached the maximum value of 42.1% at 43 °C and 56.1% at 55 °C, respectively. The highest ethylene yield of 75.5% was achieved over 0.05 wt% (500 ppm) Pd/Al_2O_3-C catalyst at the highest temperature of 105 °C. Therefore, the results suggest that at lower reaction temperatures, catalysts with higher Pd loading (such as 1%) will have better performance, whereas catalysts with much lower Pd loading (Such as 500 ppm) tend to have the best performance in ethylene yield, but at higher temperatures.

3.2 Plasma Effect on 1 wt% Pd/Al_2O_3 Catalysts

In order to understand the plasma effect on the catalysts, the 1 wt% Pd/Al_2O_3 catalysts were characterized and the results were rendered.

3.2.1 XPS Analysis

Figure 3 summarizes the XPS results of the 1 wt% Pd/Al_2O_3 catalysts with various plasma treatments in comparison to the catalyst without treatment. As shown in Fig. 3, the core level XPS spectra of Pd 3d recorded from the Pd/Al_2O_3-C sample showed two main peaks at binding energy of 342.7 and 337.3 eV, indicating of existence of only Pd^{2+} from PdO and/or Pd nitrate in the sample. In the XPS spectra of H_2 and Ar plasma treated samples, the binding energy at 341.2 and 335.7 eV was in accordance with the Pd $3d_{3/2}$ and Pd $3d_{5/2}$ of Pd^0 supported on Al_2O_3, suggesting that Pd metallic phase was formed during H_2 and Ar plasma. In addition, the XPS spectra showed that the Pd^{2+} species of the Pd/Al_2O_3-HP sample was almost not visible indicating the complete reduction of Pd^{2+} to Pd^0 during the non-thermal RF plasma treatment. With Ar plasma treatment, the surface Pd^{2+} species were partially reduced, showing shoulder peaks attributed to Pd $3d_{3/2}$ and Pd $3d_{5/2}$ of Pd^0. O_2 plasma treated Pd/Al_2O_3 sample only showed the peaks at 342.7 and 337.3 eV of Pd^{2+}, which indicated the supported Pd nitrate were not reduced during the O_2 plasma treatment. However, based on the XPS result, whether or not the supported Pd nitrate remained on the surface after

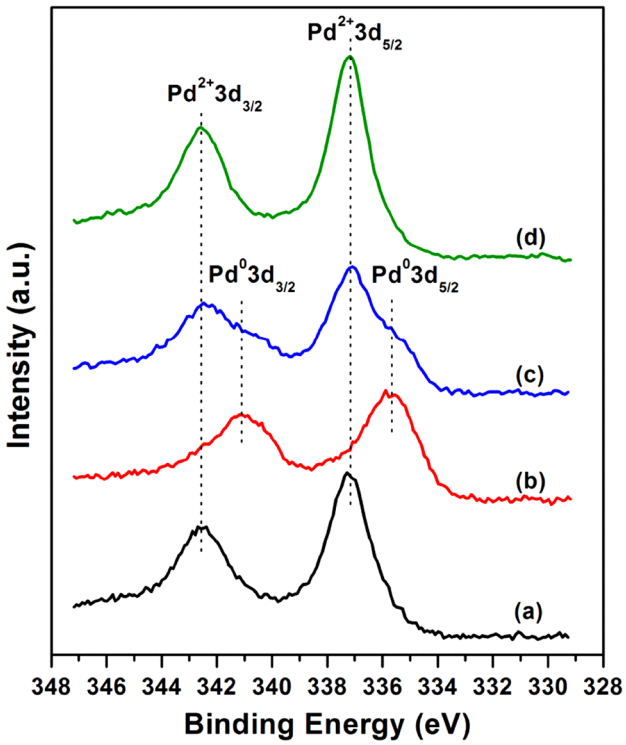

Fig. 3 XPS Pd 3d spectra of 1 wt% Pd/Al_2O_3 samples: *a* Pd/Al_2O_3-C; *b* Pd/Al_2O_3-HP; *c* Pd/Al_2O_3-AP and *d* Pd/Al_2O_3-OP

30 min of O_2 plasma treatment needs to be further confirmed by H_2-DSC.

3.2.2 H_2-DSC

DSC is a well-known technique to detect a small enthalpy change involved during the heating/cooling process. H_2-DSC has been identified as a very sensitive tool for the measurement of hydrogenation of small quantity of PdO and Pd nitrate *via* heat involved and can also differentiate their interaction with the support surfaces [31, 39]. Therefore it is expected that a methodical qualitative and quantitative study on enthalpy change involved in the hydrogen reduction of Pd precursors, including PdO and Pd nitrate, could provide useful information on the changes of the interaction between the metals/metal precursors and supports, such as the SMSI effect.

Figure 4 depicts the DSC results of 1 wt% Pd/Al_2O_3 catalysts. As shown in Fig. 4, there are two peaks of the Pd/Al_2O_3-C sample at 12.7 and 47.2 °C. The first and the second peaks of H_2-DSC analyses are assigned to the hydrogen reduction of supported PdO and $Pd(NO_3)_2$, respectively [39]. The maximum temperatures of exothermic peaks and the total heat of reduction of the samples with different plasma treatments are summarized in Table 1. T_{max1} and T_{max2} were peak temperatures of two main peaks of

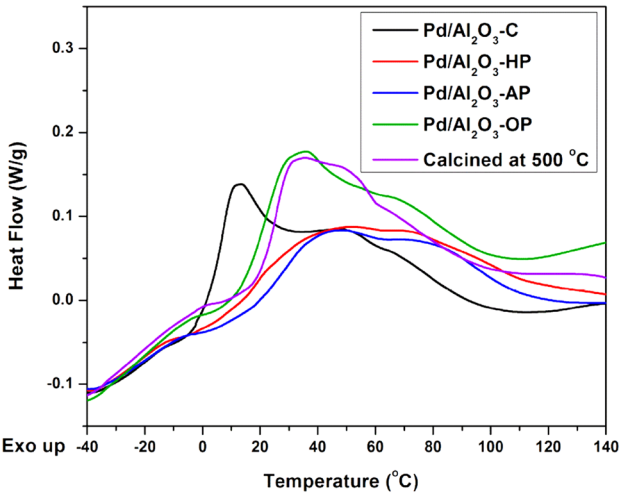

Fig. 4 H_2-DSC results of 1 wt% Pd/Al_2O_3 catalyst

each H_2-DSC result. As shown in Fig. 4 and Table 1, with 30 min of H_2 or Ar plasma treatment (Pd/Al_2O_3-HP or Pd/Al_2O_3-AP), the catalyst exhibited a single small exothermic peak around 48.3 °C while the PdO peak completely disappeared.

Normally, thermal reduction in hydrogen requires relative high temperature and an extended period of time. H_2-DSC result indicated that H_2 and Ar plasma treatment at room temperature could effectively reduce both Pd precursors, including PdO and some Pd nitrate. From the viewpoint of green chemistry principals, electrons are the best reducing agent. Specifically, electron-based reduction in RF plasma at room temperature is promising and is a straightforward way to prepare metal nanoparticles because it is an environmentally friendly, fast, and simple methodology and also is a promising alternative to hydrogen reduction at high temperatures [45]. Non-thermal RF plasma in H_2 or Ar is a potential alternative to reduce the supported metal precursors at room temperature and can avoid aggregation of Pd particles under thermal reduction conditions at high temperatures. As shown in Scheme 1, H_2 plasma could generate electrons and H•, which can work as the reducing agents and transfer autologous energy to the molecules and atoms rapidly to reduce the metal precursor. Although Ar has somewhat higher threshold electron energy of 15.76 eV for ionization, Ar^+ ions formed by electron impact ionization, containing negative ions in the discharge incorporated the change of electron density [31]. More importantly, Ar plasma treatment reduces the precursor under non-hydrogen discharge. As shown in Scheme 1 [46, 47], it is apparently to find that during H_2 and Ar plasma the generated electrons or electron-induced active species can work as the reducing agents and transfer autologous energy to the molecules and atoms rapidly to reduce the metal precursor,

Table 1 H_2-DSC, H_2-chemisorption, ethylene-TPD and the corresponding reaction results of the conventional and plasma treated 1 wt% Pd/Al_2O_3 catalyst

Sample	T_{max1} (°C)[a]	T_{max2} (°C)[a]	$\frac{\mu mol\ H_2}{g\ cat}$	D (%)[b]	d (nm)[c]	$\frac{\mu mol\ C_2H_4}{g\ cat}$	TOF (s^{-1})[d]
Pd/Al_2O_3-C	12.7	47.2	19.1	40.7	2.8	25.3	3.17
Pd/Al_2O_3-HP	–	48.4	20.5	43.6	2.7	30.5	3.85
Pd/Al_2O_3-AP	–	48.3	25.1	45.9	2.2	34.2	3.25
Pd/Al_2O_3-OP	35.3	67.0	21.6	43.6	2.6	48.5	3.06

[a]Exothermic peaks from H_2-DSC results

[b]Dispersion of Pd particles from H_2-chemisorption results

[c]Average Pd particle size from H_2-chemisorption results

[d]Metal dispersion based on H_2-chemisorption results at 25 °C

$$H_2 + e^- \longrightarrow H\cdot + H^+ + 2e^-$$
$$Ar + e^- \longrightarrow Ar^+ + 2e^-$$
$$e^- + Pd^{2+} \longrightarrow Pd$$
$$H\cdot + Pd^{2+} \longrightarrow Pd + H^+$$

$$O_2 + e^- \longrightarrow O_2^+ + 2e^-$$
$$O_2 + e^- \longrightarrow O^+ + O + 2e^-$$
$$O_2 + e^- \longrightarrow O + O^-$$
$$O_2 + e^- \longrightarrow O + O + e^-$$
$$O_2 + e^- \longrightarrow O_2^-$$
$$O + O_2 + O_2 \longrightarrow O_3 + O_2$$
$$O_2^+ + O^- \longrightarrow O_2 + O$$
$$O_3 \longrightarrow O_2 + O$$

Scheme 1 Schematic representations of plasma discharge and the active species produced

resulting in metallic phase as dispersed Pd nano-particles on the support in this case. Therefore, non-hydrogen discharge, such as Ar and He, even air can be used as the plasma generating gas for reduction [45]. With a combination of thermal treatment, excellent catalysts can be prepared in an effective way. The H_2-chemisorption and XPS spectra provide evidences of the reduction capacity and better metal dispersion of H_2 and Ar plasmas which will be further discussed below.

As shown in Fig. 4, H_2-DSC of Pd/Al_2O_3-C calcined at 500 °C also shows two distinct peaks as Pd/Al_2O_3-C. However, the PdO peak (T_{max1}) shifts to a higher temperature of 35.2 °C, with Pd nitrate peak (T_{max2}) being relatively unchanged at 50.6 °C. Similar to the H_2-DSC results of Pd/Al_2O_3-C and Pd/Al_2O_3-C calcined at 500 °C, two large exothermic peaks ascribed to the reduction of PdO and Pd nitrate appeared on the Pd/Al_2O_3-OP sample. Figure 4 shows that both the PdO and Pd nitrate peaks of Pd/Al_2O_3-C were shifted to higher temperatures by O_2 plasma treatments. With 30 min of O_2 plasma treatment, T_{max1} and T_{max2} were shifted from 12.7 and 47.2 to 35.3 and 67.0 °C, respectively, which was quite close to the sample with calcination at 500 °C. Higher reduction temperature (T_{max1} and T_{max2}) indicated stronger interaction between PdO and Pd nitrate precursors with Al_2O_3 support on the O_2 plasma treated sample. Similar strong interaction effect induced by plasma treatments were reported in the case of Pd supported on the reducible TiO_2 support [31, 39]. The H_2-DSC results in this study demonstrate that the impacts of RF O_2 plasma on modifying the interaction between precursors and supports are also effective in non-reducible support, such as Al_2O_3. It is significant that O_2 plasma could effectively produce different types of species, ions radicals and free electrons upon dissociative excitation or direct impact on excitation, such as O_2^+ and O^-, via Scheme 1 [46, 48–50]. According to earlier research by Shibata et al. [51], O^{2+} density was almost equal to the O^- density with a negligible electron density compared to the O^- density in the charge neutrality condition. Ozone (O_3) can also be produced with a wide range of electrode and discharge topologies, which is a long-lived species during the non-thermal plasma treatment and can plays an important role in modifying catalysts [52]. To be more effective, the treated catalyst should be able to interact with these very reactive species resulting in surface active structures. The dissociation of supported $Pd(NO_3)_2$ were attributed to the existence of the active oxygen species. As shown in Fig. 5, the surface Al 2p binding energy of Pd/Al_2O_3-OP exhibited a shift of 0.3 eV to higher value. It could be assumed that the active species introduced by O_2 plasma which adsorbed on the Al_2O_3 surface were bonded with the surface Al atom, concurrent with a charge transfer from the treated Al_2O_3 surface to the adsorbed O species [53]. Similar conclusion were made by Roland et al. [52], who observed the formation of a stable Al–O–O* species formed after direct plasma discharge treatment on γ-Al_2O_3. As proposed in early studies [54, 55], the electric field and active species formed by plasma could significantly change the bond distance and the structure of molecules and induce defects on the surface. Therefore, O_2 plasma could induce strong interactions between support Al_2O_3 surfaces with dissociation of supported $Pd(NO_3)_2$ under mild condition to design specific catalysts.

Overall, plasma technology, which can operate at room temperature with a plentiful of highly energetic electrons,

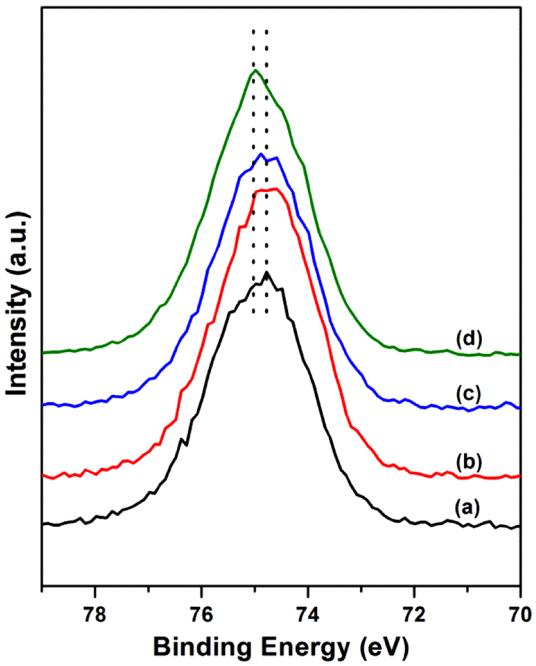

Fig. 5 XPS Al 2p spectra of 1 wt% Pd/Al_2O_3 samples: *a* Pd/Al_2O_3-C; *b* Pd/Al_2O_3-HP; *c* Pd/Al_2O_3-AP and *d* Pd/Al_2O_3-OP

is a very promising way to prepare metal nanoparticles because it is an environmentally friendly, fast, and simple methodology and also is a promising alternative to hydrogen reduction at high temperatures, avoiding the aggregation of Pd particles under thermal reduction conditions at high temperatures.

H_2-DSC experiments showed that non-thermal RF plasma treatments not only efficiently reduced the PdO and Pd nitrate precursors on the Pd/Al_2O_3 catalysts, but also induced strong interactions between support surfaces with metal precursors. XPS spectra of H_2, Ar and O_2 plasma treated samples also confirmed the H_2-DSC results.

3.2.3 H_2-Chemisorption

The hydrogen uptake values of 1 wt% Pd/Al_2O_3 catalysts obtained from the hydrogen pulse chemisorption are summarized in Table 1 along with the results of Pd dispersion and Pd particle size. Although Pd can easily absorb large amounts of hydrogen through gas loading, which results in the formation of palladium hydrides, the hydrogen pulse chemisorption in this work were carried out under the same procedure. In order to compare the effect of plasma treatment on the catalyst precursor, the average dispersion of palladium crystallites was determined by the stoichiometic factor $H_2/Pd = 0.5$ on the all the samples.

Plasma treated samples showed better dispersion than the conventional sample, which indicated non-thermal RF plasma treatment could improve the Pd dispersion, as reported before [56]. The particle sizes of plasma treated samples were smaller than those of the conventionally H_2-reduced counterpart, indicating that plasma reduction is effective in enhancing the distribution of metal nanoparticles. Argon plasma showed the best enhancement in Pd dispersion among the three plasma treated samples. The possible mechanism of RF plasma reduction resulting in higher metal dispersion is that plasma treatment introduces high energy species, such as electrons and ions, which are very strong reducing species, and can act as reducing agent to reduce Pd^{2+} to Pd^0. The reduced Pd could retain some electric charge and repel each other, resulting in the uniform dispersion of Pd particles in the catalyst structure [57].

3.2.4 C_2H_4-TPD

The sub-ambient temperature-programmed desorption (TPD) of ethylene results are depicted in Fig. 6 and summarized in Table 1. The total amount of ethylene adsorbed was similar for all the samples. However, the peaks of ethylene-TPD from the catalyst surface appeared at different temperatures likely depending on the adsorbed forms on the catalysts. As reported in the literatures [15, 58, 59], ethylene could adsorb on the Pd surface in π or di-σ modes. In the π-bonded chemisorption mode, ethylene stood atop the single Pd atom. In the di-σ mode, ethylene bonded parallel to one of the bridge Pd–Pd bonds forming two σ-palladium-carbon bonds, as illustrated in Fig. 6. It is generally accepted that the high temperature peak is assigned to di-σ-bonded ethylene on Pd and the low temperature peak is assigned to π-bonded ethylene on Pd, which is more weakly adsorbed and consequently deso[rbed without decomposition [15]. The peak at 33.1 °C of Pd/Al_2O_3-C was assigned to di-σ-bonded ethylene which could undergo dehydrogenation during TPD. As shown in Fig. 6 and Table 1, with H_2 and Ar plasma treatments, the ethylene mainly adsorbed on Pd in π-bonded state. In the case of O_2 plasma sample, the peak is assigned to di-σ-bonded adsorption and is shifted to lower temperature of at 9.5 °C compared to the conventional sample Pd/Al_2O_3-C. From the ethylene-TPD results, the change of ethylene adsorption, from di-σ-bonded state to surface π-bonded adsorption and the shift to lower temperature for desorption could be attributed to the stronger interaction between Pd particles and the Al_2O_3 support. Similar effects of plasma treatment had been observed in our previous studies on Pd/TiO_2 [31].

It is generally accepted that alkenes hydrogenation follows the classical Horiuti-Polanyi mechanism. This reaction scheme involves the sequential hydrogenation of acetylene and its subsequent hydrocarbon intermediates, thus resulting in the desired ethylene and undesired ethane products [15, 60–62]. The acetylene hydrogenation reaction

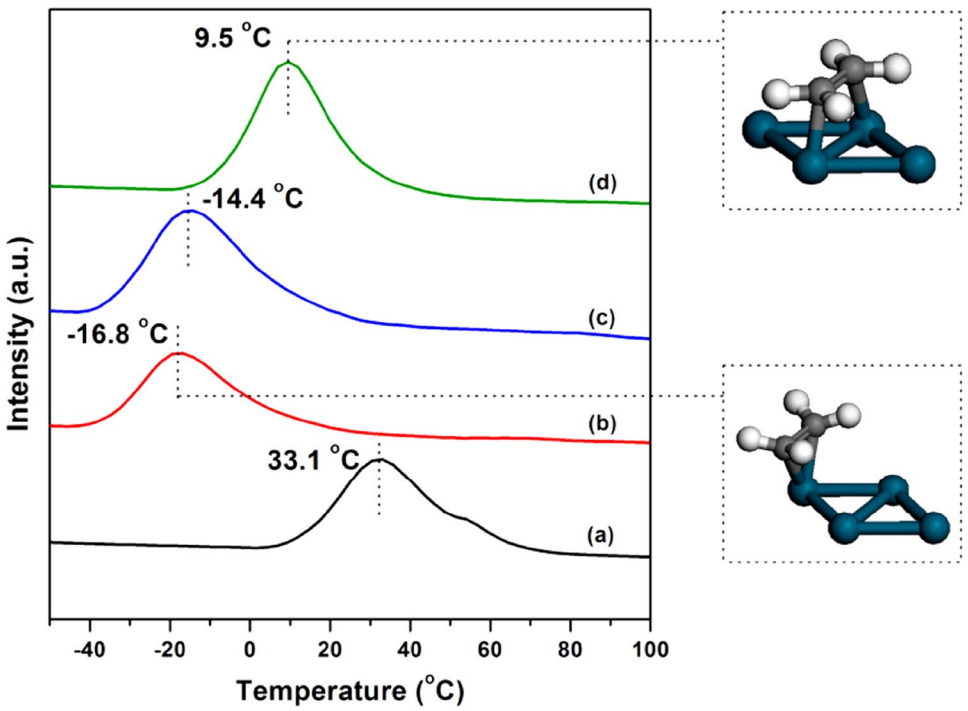

Fig. 6 Ethylene-TPD of 1 wt% Pd/Al_2O_3 samples: *a* Pd/Al_2O_3-C; *b* Pd/Al_2O_3-HP; *c* Pd/Al_2O_3-AP and *d* Pd/Al_2O_3-OP

will proceed via the pathway of acetylene to ethylene and then ethane. Therefore, the ethylene-TPD was carried out and the results were shown that different adsorption type of ethylene on Pd could consequently result in the different behavior of ethylene selectivity. The di-σ-bonded intermediate is considered to be more stable leading to strong interaction and a strong distortion of ethylene toward the sp^3 hybridization to the formation of over-hydrogenated products ethane, whereas the π-bonded species are with less interaction easily desorbed as ethylene molecules [63]. The ethylene-TPD results show that the Pd/Al_2O_3-HP and Pd/Al_2O_3-AP samples mainly exhibited π-bonded adsorption of ethylene. Consequently, it can be assumed that the reason the plasma treated catalysts achieving better acetylene activity and ethylene selectivity is due to favorable adsorption of acetylene on catalysts after plasma treatments.

3.2.5 Reaction Test

The characterization results above confirm that the plasma treatment for the 1 wt% Pd/Al_2O_3 catalysts could induce strong metal-support interaction with better Pd dispersion. Figure 7 summarizes the results of acetylene conversion and selectivity to ethylene of the Pd/Al_2O_3 catalysts with the pre-reduction at 200 °C for 30 min. As shown in Fig. 7a, the conversion of acetylene of all samples increases with temperature. The initial conversion of Pd/Al_2O_3-C sample was about 16.3% at 25 °C, and increased to 98.9% with the elevated temperature. While the T_{50} values for the hydrogenation reaction on the conventional catalysts was 37.5 °C, the corresponding T_{50} values for the hydrogenation reaction on the catalysts with O_2, H_2 and Ar plasma treatment were 33.3, 35.2 and 35.3 °C, respectively. The catalyst performance of plasma treated catalysts was significantly improved, exhibiting the acetylene conversion sequence as: Pd/Al_2O_3-OP > Pd/Al_2O_3-HP > Pd/Al_2O_3-AP > Pd/Al_2O_3-C for lower temperature range of 29–37 °C. At temperature higher than 37 °C, the catalysts prepared by plasma methods exhibited a higher activity at the same temperatures, compared to the conventional catalyst. The activities order of these catalysts is: Pd/Al_2O_3-HP > Pd/Al_2O_3-AP > Pd/Al_2O_3-OP > Pd/Al_2O_3-C. In all cases, acetylene was hydrogenated up to nearly 100% conversion at or above 49 °C over the catalysts with the H_2 and Ar plasma treatments. Therefore, with plasma treatment, the acetylene hydrogenation activities show better performance than that of the conventional sample Pd/Al_2O_3-C, which is in line with the Pd dispersion on the catalysts.

Figure 7b shows the ethylene selectivity on the catalysts with respect to the reaction temperature. As reported before, the selectivity for ethylene could be very low, sometimes crossing over from positive to negative with a large amount of ethane formed [64]. Based on the previous results on the Pd/TiO_2 catalysts with similar plasma treatments [31], the non-thermal RF plasma in H_2 or Ar is an effective alternative to reduce the supported Pd species at room temperature while O_2 plasma introduced the strong metal-support interaction on the TiO_2 surface. The SMSI effect accompanied by the presence of Ti^{3+} on the reducible support TiO_2 has been confirmed to be a key factor

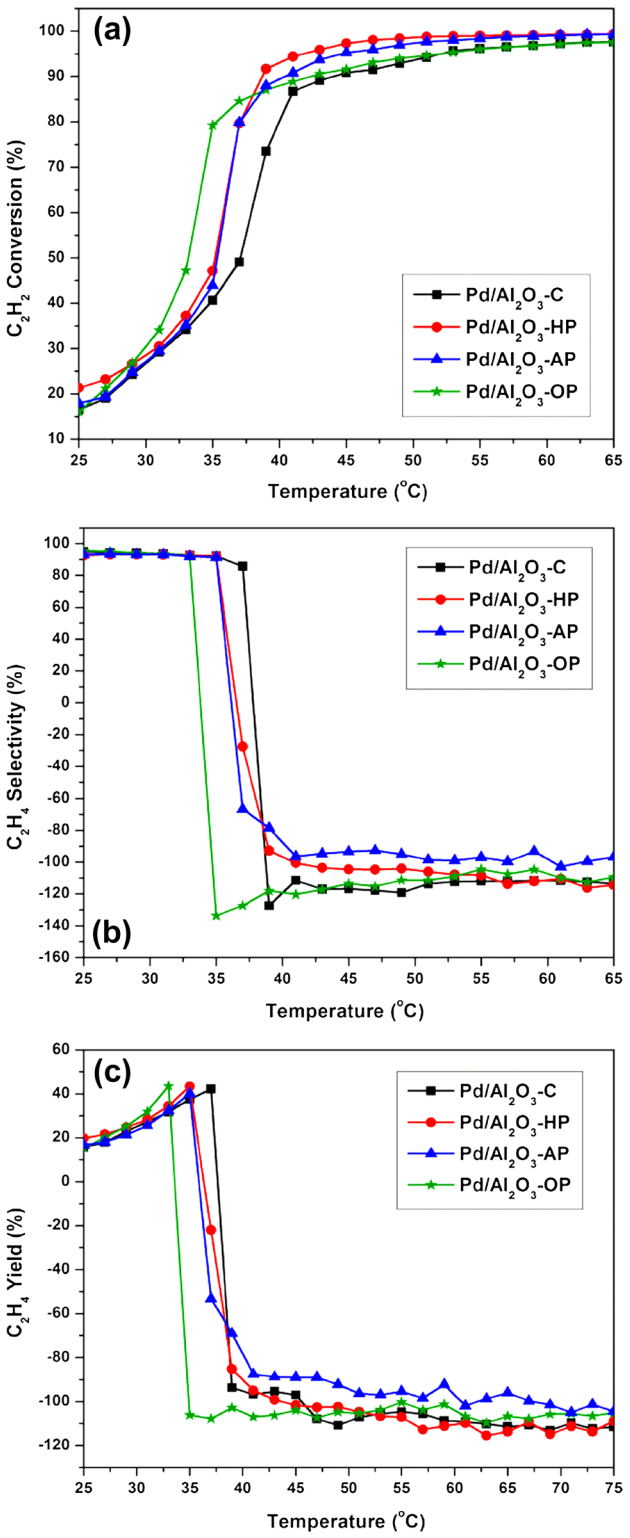

Fig. 7 Catalytic performance including **a** conversion, **b** selectivity and **c** yield of 1 wt% Pd/Al_2O_3 catalyst with H_2, Ar, and O_2 plasma treatment and the conventional counterpart. GHSV = 90,000 mL/h/g with the H_2/C_2H_2 ratio of 3/1

for the enhanced ethylene selectivity. The reducibility of the Ti^{4+} to Ti^{3+} species and the subsequent mobility of oxygen species, favored by the strong metal-support interaction, increase the surface oxygen vacancy concentration [65]. It is commonly accepted that reducible or partially reducible supports lead to strong metal-support interaction much easier than non-reducible supports. In this study, although Al_2O_3 has been identified as non-reducible support, it is clearly shown that the strong interaction between the Al_2O_3 support and Pd precursor and particles can be readily induced by plasmas, as evidenced by the results in the H_2-DSC, H_2-chemisorption and ethylene-TPD sections. The plasma treatment not only considerably reduces $Pd(NO_3)_2$ to Pd metal, but also strengthens the interaction between the precursor and the Al_2O_3 support, which could enhance the desorption of ethylene. In comparison to the conventional Pd/Al_2O_3 catalyst, plasma treated samples exhibit improved acetylene activity and ethylene selectivity in the whole temperature range investigated. As shown in Fig. 7b, at 37 °C, the selectivity order of these catalysts is: Pd/Al_2O_3-C > Pd/Al_2O_3-HP > Pd/Al_2O_3-AP > Pd/Al_2O_3-OP. The better selectivity performance of the conventional sample was contributed to the higher desorption temperature of ethylene on Pd/Al_2O_3-C. Since the ethylene desorption on Pd/Al_2O_3-C required higher temperature than the plasma treated samples, at 37 °C, the ethylene on the conventional sample has not desorbed yet. However, once it hit the ethylene desorption temperature, the selectivity dropped dramatically, and then the selectivity of Pd/Al_2O_3-C was lower than those of the plasma treated samples. Pd/Al_2O_3-HP and Pd/Al_2O_3-AP exhibit higher ethylene selectivity than the O_2 plasma treated sample, which could be attributed to the weakened ethylene adsorption strength on the Pd surface. *TOF* values were calculated at 25 °C and expressed as the rate of acetylene consumption per number of exposed Pd sites on the four catalyst samples. As given in Table 1, Pd/Al_2O_3-HP exhibited the highest *TOF*s (3.85 s^{-1}) among all the catalysts

Plasma treatment was also applied to the 0.05 wt% (500 ppm) Pd/Al_2O_3 samples in order to enhance the catalytic performance. The comparison results of acetylene conversion, ethylene selectivity and yield over 0.05 wt% (500 ppm) Pd/Al_2O_3 samples are summarized in Fig. 8. Compared to the results in Fig. 7, the conversion of acetylene of 0.05 wt% (500 ppm) Pd/Al_2O_3-HP sample is not as good as the catalyst with 1 wt% Pd loading, suggesting the enhancement of plasma treatment would be influenced by the metal loading and dispersion on the support. As shown in Figs. 3 and 4, H_2 plasma treatment could efficiently reduce the supported $Pd(NO_3)_2$ at room temperature. The reaction results showed that reduction process for the Pd/Al_2O_3-HP sample might enhance the particle size by aggregation of dispersed Pd particles, which is not favorable for

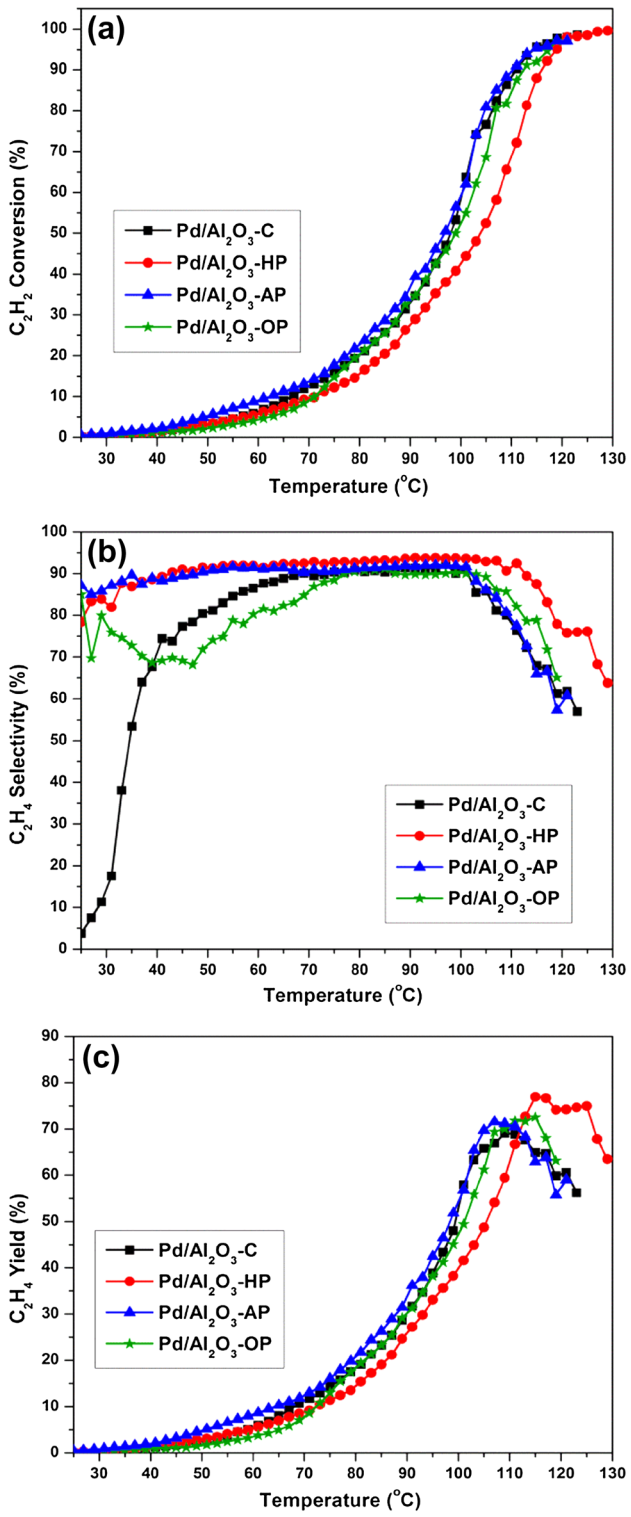

Fig. 8 Catalytic performance including **a** conversion, **b** selectivity and **c** yield of 0.05 wt% (500 ppm) Pd/Al_2O_3 catalyst with H_2, Ar, and O_2 plasma treatment and the conventional counterpart. Without pre-reduction, GHSV = 90,000 mL/h/g with the H_2/C_2H_2 ratio of 3/1

the hydrogenation of acetylene to ethylene [7]. With H_2 and Ar plasma treatment, the catalysts had Pd metal on the surface and showed enhanced selectivity performance apparently.

In Fig. 8, without pre-reduction, conventional sample and O_2 plasma treated sample require some activity initiation and then they reach constant selectivity of 90.0% around 75 °C. The selectivity of the conventional 0.05 wt% (500 ppm) Pd/Al_2O_3 samples without pre-reduction was at about 91.0% until the temperature rising up to 70 °C and then dropped when the temperature was above 100 °C. As shown in Figs. 3 and 4, H_2 and Ar plasma treatment could efficiently reduce the supported $Pd(NO_3)_2$ at room temperature. Therefore, in Fig. 8b, it shows that the Pd/Al_2O_3-HP and Pd/Al_2O_3-AP exhibit higher ethylene selectivity than the O_2 plasma treated sample. Also, among the four counterparts, Pd/Al_2O_3-AP achieves the best maximum ethylene yield of 76.9% at about 105 °C. The enhancement differences of 1 wt% Pd/Al_2O_3 catalyst and 0.05 wt% Pd/Al_2O_3 catalyst will be further investigated in future studies.

4 Conclusions

Pd/Al_2O_3 catalysts were investigated for selective hydrogenation of acetylene to ethylene. Reaction with higher H_2/C_2H_2 ratio favored higher acetylene conversion but with lower ethylene selectivity. Non-thermal RF plasma treatment were employed in the catalyst preparation procedure, and the effect of RF plasma treatment on the catalytic performance of Pd/Al_2O_3 catalysts with different Pd loading in selective acetylene hydrogenation were also investigated in this work. It is demonstrated that RF plasma in H_2 or Ar is an efficient alternative to reduce the supported Pd species at room temperature and can avoid aggregation of Pd particles under thermal reduction conditions at high temperatures. With O_2 plasma treatment, the catalysts showed strong interaction between the non-reducible Al_2O_3 support and PdO/Pd nitrate precursors as well, which is evidenced by the H_2-DSC, H_2-chemisorption and ethylene-TPD results. Plasma treated Pd/Al_2O_3 catalysts appeared to promote ethylene selectivity, mainly due to the enhanced desorption of ethylene, in selective acetylene hydrogenation in comparison with the untreated counterpart catalyst. The detailed enhancement effect of plasma on Pd/Al_2O_3 catalyst with different Pd loading will be better understood in future industrial studies.

Acknowledgements The financial support of the NSF-REU program at TAMU-Commerce and Welch Foundation (Grant # T-0014) is acknowledged. A portion of this research was conducted at the Center for Nanophase Materials Sciences, sponsored at Oak Ridge National Laboratory (CNMS-ORNL User Project).

References

1. Liu D (2016) Appl Surf Sci 386:125–137
2. Yang B, Burch R, Hardacre C, Hu P, Hughes P (2016) Surf Sci 646:45–49
3. Crespo-Quesada M, Yoon S, Jin M, Xia Y, Weidenkaff A, Kiwi-Minsker L (2014) ChemCatChem 6:767–771
4. Bazzazzadegan H, Kazemeini M, Rashidi AM (2011) Appl Catal A 399:184–190
5. Yan X, Bao J, Yuan C, Wheeler J, Lin WY, Li R, Jang BWL (2016) J Catal 344: 194–201
6. Borodziński A, Bond GC (2006) Catal Rev 48: 91–144
7. Borodziński A, Bond GC (2008) Catal Rev 50: 379–469
8. Oliver RG, Wells PB (1977) J Catal 47:364–370
9. Crampton AS, Rötzer MD, Schweinberger FF, Yoon B, Landman U, Heiz U (2016) J Catal 333: 51–58
10. Zhang H, Yang Y, Dai W, Lu S, Yu H, Ji Y (2014) Chin J Chem Eng 22:516–521
11. Benavidez AD, Burton PD, Nogales JL, Jenkins AR, Ivanov SA, Miller JT, Karim AM, Datye AK (2014) Appl Catal A 482:108–115
12. Zhang Y, Diao W, Williams CT, Monnier JR (2014) Appl Catal A 469:419–426
13. Kim E, Shin EW, Bark CW, Chang I, Yoon WJ, Kim W-J (2014) Appl Catal A 471:80–83
14. Kim SK, Lee JH, Ahn IY, Kim W-J, Moon SH (2011) Appl Catal A 401:12–19
15. Mei D, Sheth PA, Neurock M, Smith CM (2006) J Catal 242:1–15
16. Borodziński A, Cybulski A (2000) Appl Catal A 198:51–66
17. Albers P, Seibold K, Prescher G, Müller H (1999) Appl Catal A 176:135–146
18. Karakhanov E, Maximov A, Kardasheva Y, Semernina V, Zolotukhina A, Ivanov A, Abbott G, Rosenberg E, Vinokurov V (2014) ACS Appl Mater Interfaces 6:8807–8816
19. Long W, Brunelli NA, Didas SA, Ping EW, Jones CW (2013) ACS Catal 3:1700–1708
20. Park J, Joo J, Kwon SG, Jang Y, Hyeon T (2007) Angew Chem Int Ed 46:4630–4660
21. Yuan Y, Yan N, Dyson PJ (2012) ACS Catal 2:1057–1069
22. Layan Savithra GH, Bowker RH, Carrillo BA, Bussell ME, Brock SL (2013) ACS Appl Mater Interfaces 5:5403–5407
23. Tsung C-K, Fan J, Zheng N, Shi Q, Forman AJ, Wang J, Stucky GD (2008) Angew Chem Int Ed 47:8682–8686
24. Wirth S, Harnisch F, Quade A, Brüser M, Brüser V, Schröder U, Savastenko NA (2011) Plasma Processes Polym 8:914–922
25. Liu C-J, Vissokov GP, Jang BWL (2002) Catal Today 72:173–184
26. Li Y-N, Xie Y-B, Liu C-J (2008) Catal Lett 125:130–133
27. Nozaki T, Hiroyuki T, Okazaki K (2005) Energy Fuels 20:339–345
28. Stere C E, Adress W, Burch R, Chansai S, Goguet A, Graham W G, De Rosa F, Palma V, Hardacre C (2014) ACS Catal 4:666–673
29. Liu X, Li Y, Lee JW, Hong C-Y, Mou C-Y, Jang BWL (2012) Appl Catal A 439–440:8–14
30. Zhou T, Jang K, Jang BWL (2013) Catal Today 211:147–155
31. Li Y, Jang BWL (2011) Appl Catal A 392:173–179
32. Ratanatawanate C, Macias M, Jang BWL (2005) Ind Eng Chem Res 44:9868–9874
33. Yan X, Zhao B, Liu Y, Li Y (2015) Catal Today 256:29–40
34. Yan X, Li S, Bao J, Zhang N, Fan B, Li R, Liu X, Pan YX (2016) ACS Appl Mater Interfaces 8:17060–17067
35. Lee SW, Mattevi C, Chhowalla M, Sankaran RM (2012) J Phys Chem Lett 3:772–777
36. Wang J, Wang Z, Liu C-J (2014) ACS Appl Mater Interfaces 6:12860–12867
37. Khataee A, Bozorg S, Khorram S, Fathinia M, Hanifehpour Y, Joo SW (2013) Ind Eng Chem Res 52:18225–18233
38. Wang Z, Yang RT (2010) J Phys Chem C 114:5956–5963
39. Li Y, Jang BWL (2010) Ind Eng Chem Res 49:8433–8438
40. Amorim C, Keane MA (2008) J Colloid Interface Sci 322:196–208
41. Duca D, Frusteri F, Parmaliana A, Deganello G (1996) Appl Catal A 146:269–284
42. Cui X, Zhou X, Chen H, Hua Z, Wu H, He Q, Zhang L, Shi J (2011) Int J Hydrog Energy 36:10513–10521
43. Sheth PA, Neurock M, Smith CM (2003) J Phys Chem B 107:2009–2017
44. He Y-F, Feng J-T, Du Y-Y, Li D-Q (2012) ACS Catal 2:1703–1710
45. Liu C-J, Zhao Y, Li Y, Zhang D-S, Chang Z, Bu X-H (2014) ACS Sustain Chem Eng 2:3–13
46. Seo H, Kim J-H, Shin Y-H, Chung K-H (2004) J Appl Phys 96:6039–6044
47. Wang W-G, Xu Y, Yang X-F, Wang W-C, Zhu A-M (2005) Rapid Commun Mass Spectrom 19:1159–1166
48. Kim HY, Kang SK, Kwon HC, Lee HW, Lee JK (2013) Plasma Processes Polym 10:686–697
49. Tomoyuki M, Kari N, Timo G, Deborah OC, William GG (2013) Plasma Sources Sci Technol 22:045010
50. Parvulescu VI, Magureanu M, Lukes P (2012) Plasma chemistry and catalysis in gases and liquids. Wiley-VCH Verlag & Co. KGaA, Weinheim
51. Shibata M, Nakano N, Makabe T (1996) J Appl Phys 80:6142–6147
52. Roland U, Holzer F, Kopinke FD (2005) Appl Catal B 58:217–226
53. McBriarty ME, Campbell GP, Drake TL, Elam JW, Stair PC, Ellis DE, Bedzyk MJ (2015) J Phys Chem C 119:16179–16187
54. Liu C-J, Zou J, Yu K, Cheng D, Han Y, Zhan J, Ratanatawanate C, Jang BWL (2006) Pure Appl Chem 78:1227–1238
55. Achtyl JL, Vlassiouk IV, Dai S, Geiger F (2014) J Phys Chem C 118:17745–17755
56. Zea H, Chen C-K, Lester K, Phillips A, Datye A, Fonseca I, Phillips J (2004) Catal Today 89:237–244
57. Belloni J (2006) Catal Today 113:141–156
58. Stuve EM, Madix RJ (1985) J Phys Chem 89:105–112
59. Zhu B, Jang BWL (2014) J Mol Catal A 395:137–144
60. Gaube J, Klein HF (2014) Appl Catal A 470:361–368
61. Segura Y, López N, Pérez-Ramírez J (2007) J Catal 247:383–386
62. Li J-N, Pu M, Ma C-C, Tian Y, He J, Evans D G (2012) J Mol Catal A 359:14–20
63. Fahmi A, van Santen RA (1996) J Phys Chem 100: 5676–5680
64. Liu X, Mou C-Y, Lee S, Li Y, Secrest J, Jang B W L (2012) J Catal 285:152–159
65. Durgasri DN, Vinodkumar T, Lin F, Alxneit I, Reddy BM (2014) Appl Surf Sci 314:592–598